



A novel framework for vegetation change characterization from time series landsat images



Hancheng Guo^{a,1}, Yanyu Wang^{a,1}, Jie Yu^b, Lina Yi^c, Zhou Shi^{a,d}, Fumin Wang^{a,*}

^a Institute of Agricultural Remote Sensing and Information Technology Application, College of Environmental and Resource Sciences, Zhejiang University, Hangzhou, 310058, China

^b Zhejiang Ecological and Environmental Monitoring Center, Hangzhou, 310012, China

^c Environmental Development Center of the Ministry of Ecology and Environment, Beijing, 100029, China

^d Key Laboratory of Spectroscopy Sensing, Ministry of Agriculture, Hangzhou, 310058, China

ARTICLE INFO

Handling Editor: Aijie Wang

Keywords:

Vegetation
NDVI
Framework
Disturbance
Change detection

ABSTRACT

Understanding terrestrial ecosystem dynamics requires a comprehensive examination of vegetation changes. Remote sensing technology has been established as an effective approach to reconstructing vegetation change history, investigating change properties, and evaluating the ecological effects. However, current remote sensing techniques are primarily focused on break detection but ignore long-term trend analysis. In this study, we proposed a novel framework based on a change detection algorithm and a trend analysis method that could integrate both short-term disturbance detection and long-term trends to comprehensively assess vegetation change. With this framework, we characterized the vegetation changes in Zhejiang Province from 1990 to 2020 using Landsat and landcover data. Benefiting from combining break detection and long-term trend analysis, the framework showcased its capability of capturing a variety of dynamics and trends of vegetation. The results show that the vegetation was browning in the plains while greening in the mountains, and the overall vegetation was gradually greening during the study period. By comparison, detected vegetation disturbances covered 57.71% of the province's land areas (accounting for 66.92% of the vegetated region) which were mainly distributed around the built-up areas, and most disturbances (94%) occurred in forest and cropland. There were two peak timings in the frequency of vegetation disturbances: around 2003 and around 2014, and the proportions of more than twice disturbances in a single location were low. The results illustrate that this framework is promising for the characterization of regional vegetation growth, including long-term trends and short-term features. The proposed framework enlightens a new direction for the continuous monitoring of vegetation dynamics.

1. Introduction

In recent years, the greenhouse effect and carbon neutralization were widely studied by social circles because of the great pressure brought on by climate change (Danneyrolles et al., 2019). Vegetation plays a significant role in terrestrial ecosystems, and changes in vegetation can reflect the evolution of regional climate and ecosystems (Li et al., 2019; Soudzilovskaya et al., 2019; Wang et al., 2021). Therefore, many studies have explored the changing characteristics of vegetation on regional, national to global scales. For instance, Nguyen et al. (2018) proposed an approach to comprehensively define and assess long-term forest dynamics for sustainable forest management and climate change mitigation; Novillo et al. (2019) assessed the ecosystem resilience in Central

Asia by using the NDVI variation; Benedict et al. (2021) used the satellite-based time series of vegetation index to monitor the trend of drought area as an indicator of climate change. With the increasing impact of anthropogenic activities on ecosystems and the increase of extreme natural disasters, the growth of vegetation was disturbed more frequently and dramatically (Ge et al., 2021). Therefore, monitoring long-term vegetation dynamics and identifying spatiotemporal characteristics of vegetative changes hold great importance to ecological conservation.

With numerous vegetation indices such as the Normalized Difference Vegetation Index (NDVI), the Enhanced Vegetation Index (EVI), and the Leaf Area Index (LAI), using remote sensing data to monitor the changes in vegetation has become an indispensable tool for studies relating to

* Corresponding author.

E-mail address: wfm@zju.edu.cn (F. Wang).

¹ These authors contributed equally to this work and should be considered co-first authors.

global climate change and macro-ecological change (Fu et al., 2022; Lin et al., 2020; Liu et al., 2022). However, most related studies mainly focused on the long-term trends of vegetation. For example, Liang et al. (2020) explored ecological change by examining spatiotemporal dynamics of vegetation change in an artificial desert oasis in Northwest China; Novillo et al. (2019) analyzed the temporal statistical trends of the NDVI to explore whether there are differences, by hydroclimatic type, in mainland Spain and the Balearic Islands; Wei et al. (2018) used four remote sensing-based indices to represent changes in vegetation cover in forest-dominated regions worldwide.

Reviewing the relevant studies that have already been performed, we considered that these researches focused more on describing the long-term trend of vegetation changes, emphasizing the growth situation of the whole vegetation in areas, but this is not intact for analysis of vegetation growth. Because apart from the long-term trend, abrupt disturbances, which frequently be missed in the long-term trend analysis as be averaged and overshadowed, could reflect changes that occurred during vegetation growth as well. The analysis of vegetation change detection requires more remote sensing images, higher image resolution and powerful computing power, and the complete process has not been gradually improved until recent years.

Some innovative algorithms have been developed for change detection in recent years. Among the emerging methods, three algorithms are widely accepted and applied: the Breaks For Additive Seasonal and Trend (BFAST) algorithm (Fang et al., 2018; Verbesselt et al., 2010), the LandTrendr algorithm (Kennedy et al., 2010), and the Continuous Degradation Detection (CCDC) algorithm (Zhu and Woodcock, 2014). These approaches could be applied to determine the breakpoint years, disturbance duration, and intensity of vegetation disturbances (Bueno et al., 2020), which further help characterize the vegetation change comprehensively (Komba et al., 2021).

At present, the commonly used sources of remote sensing data for vegetation studies include Moderate-resolution Imaging Spectroradiometer (MODIS), and Landsat (Li et al., 2021; Radocaj et al., 2020). Selecting the appropriate sensor is important for vegetation studies since each of them has unique spatial, temporal, spectral, and radiometric properties (Zhu et al., 2022). As for the MODIS, even though it has a 12-h resampling rate for the same area, its data has been officially released since April 2000, and it is difficult to meet the needs of this study. In addition, the highest spatial resolution of MODIS is 250 m, and the images may have some null values (Tao et al., 2019). In contrast, Landsat is the longest-running Earth observation system, with a long-time sequence (50 years) of image data collection history, and a higher spatial resolution (30 m), suitable for large time-span analysis. Moreover, Landsat images have more bands and have excellent quality outstanding geometric and radiometric calibration quality (Hemati et al., 2021; Woodcock et al., 2008; Wulder et al., 2019). In summary, MODIS images are better suited for studies with wide research regions and low image precision requirements whereas Landsat images are better suited for studies with high image precision needs and long-term time sequences. Therefore, we chose to use Landsat images in this study.

In this case, we proposed a novel framework consisting of a change detection algorithm and a trend analysis method to more comprehensively characterize the vegetation change. The main purpose of this study is to illustrate the complete structure and operation process of this framework. The algorithms and data selected by this framework are mature and complete and have high rationality. Specially, to better explain this framework, we implemented the framework on the Google Earth Engine (GEE) platform and applied it for mapping vegetation change in Zhejiang province in China.

2. Materials and methods

2.1. Study area

The study region ($118^{\circ}01' - 123^{\circ}10' \text{ E}$, $27^{\circ}02' - 31^{\circ}11' \text{ N}$) is the

whole Zhejiang Province, located on the southeast coast of China and the southern part of the Yangtze River Delta, with a total size of 105,500 square kilometers (Fig. 1). The terrain in the study region is undulating, with mountains and hills accounting for about 74.63% of the province's total area, and the climate type is subtropical humid monsoon climatic with ample sunlight and rainfall. Therefore, Zhejiang Province is rich in vegetation resources, and the forest coverage rate achieves 60% (He et al., 2020). The main type of vegetation is subtropical evergreen broad-leaved forest, and the crop is dominated by single-cropping rice (Fig. S1). Meanwhile, the major population concentrates on the eastern coast, plains in the north, and central land area with cultivated land areas close to 16,000 square kilometers.

Zhejiang Province always insists on developing ecological civilization construction vigorously. However, human activities, including urban sprawl, road construction, and the opening up of wasteland, may lead to the resilience decrease of an ecosystem, especially for vegetation (Zhang and Huang, 2019). As a typically developed region in China, the evolution of vegetation in Zhejiang Province could reflect the changes in the terrestrial ecosystem under the combined effects of human activities and climate change.

2.2. Data sources

2.2.1. Remote sensing data

The spectral reflectance of the surface changes can reflect the biophysical, and ecological processes on the land surface (Houborg et al., 2007). Various change processes, such as vegetative regrowth, disturbances, and climate variability, may trigger different temporal signals from the satellite-based time series. To ensure adequate temporal density for trend analysis, we used all available Landsat-5 TM, Landsat-7 ETM+, and Landsat-8 OLI images acquired between 1990 and 2020. To assure the inter-sensing harmonization and temporal continuity between Landsat sensors, we also conducted spectral transformation between OLI and ETM + using the coefficients suggested by Roy et al. (2016).

2.2.2. The landcover dataset

To better analyze the spatiotemporal changes of the vegetation, and keep the resolution of Landcover data and NDVI consistent, this study used the China Land Cover Dataset (CLCD) dataset (Yang and Huang, 2021). The period of the CLCD dataset is from 1990 to 2020 with a spatial resolution of 30 m. The CLCD dataset contains 5 different classifications of vegetation types, including cropland, forest, shrub, grassland, and wetland (Fig. S2).

2.2.3. The statistical data

This study used the forestry and agricultural data from the statistical yearbooks of the Zhejiang Provincial Bureau of Statistics during the study period to more effectively demonstrate the correctness of the results.

2.3. Methods

This framework consists of three sequentially integrated sections: the pre-processing module, the change characteristic analysis module, and the comparative analysis module (Fig. 2). In the first part, we pre-processed the Landsat SR data and CLCD dataset, to generate an NDVI dataset and a landcover dataset. All the cloud pixels in Landsat images have been masked and non-vegetated pixels were removed as well. The second part characterized the vegetation changes by dividing the long-term vegetation time series into a trend part and a short-term disturbance part. Meanwhile, we quantified disturbances that are critical for understanding ecosystem dynamics. Compared to previous studies (Hermosilla et al., 2019; Zhou et al., 2019), we extracted more vegetation disturbance characteristic parameters such as the disturbance area statistics for county-level divisions, and the annual disturbance area of

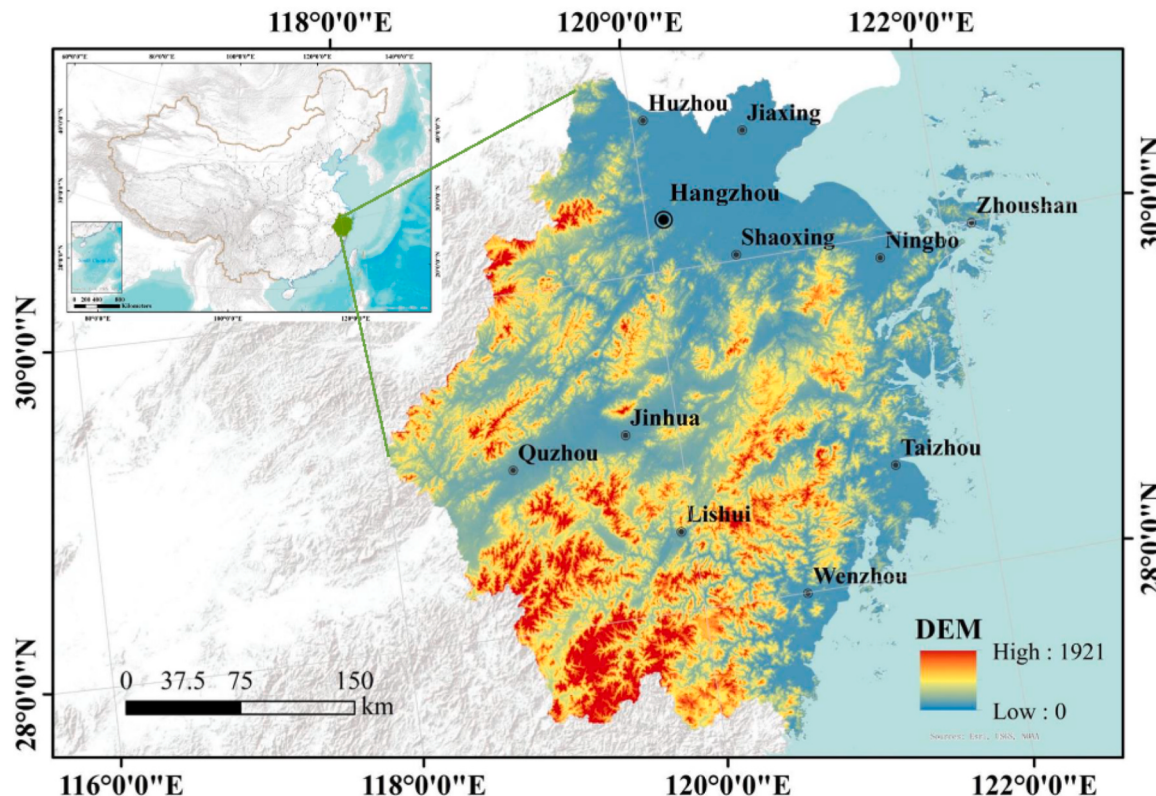


Fig. 1. The location and topography of the study area.

different types of vegetation; both of which could improve the accuracy of disturbance analysis and enhance the ability to supplement the long-term change trend. Additionally, the description of vegetation disturbance characteristics are more detailed, such as the frequencies of disturbance, disturbed areas of different types of vegetation cover, etc. Finally, we obtained the trend and disturbance characteristics of vegetation over the study area, and we applied a comparative analysis to compare the two types of vegetation features.

2.3.1. Pre-processing module

We used the Quality Assessment (QA) Band generated by the C Function of Mask algorithm for cloud removal, which improves the integrity of scientific research by marking which pixels may be affected by instruments or clouds. The CFMask algorithm uses decision trees to prospectively label pixels in the scene, and then, those labels are validated or discarded according to scene-wide statistics. Because this algorithm is derived from a priori knowledge of physical phenomena and is operable without geographic restriction, it can be used for current and future land imaging missions (Foga et al., 2017).

Normalized Difference Vegetation Index (NDVI), which is widely used in remote sensing applications, is one of the important spectral parameters for monitoring vegetation growth. This study used the NDVI index to analyze the long-term trends. The maximum value composite (MVC) method (Holben, 1986) was applied to obtain a yearly NDVI in the growing season (June to September). Also, we established a threshold ($NDVI > 0.2$) to reduce the noise from non-vegetation signals. The NDVI is calculated as:

$$NDVI = (NIR - R) / (NIR + R) \quad (1)$$

where NIR represents near-infrared reflectance, and R represents red reflectance.

Additionally, we used the Normalized Burn Ratio (NBR) index to analyze vegetation disturbance because NBR is proven to be better

suitable for detecting disturbance-related vegetation change, particularly on structural change (Hislop et al., 2019). NBR is defined as:

$$NBR = (NIR - SWIR1) / (NIR + SWIR1) \quad (2)$$

where NIR denotes near-infrared reflectance ($0.85\text{--}0.88\text{ }\mu\text{m}$), and SWIR denotes short-wave infrared ($1.57\text{--}1.65\text{ }\mu\text{m}$). All the remote sensing data were processed on the GEE platform and ArcGIS 10.3.

2.3.2. Long-term trend analysis and change detection

2.3.2.1. Long-term trend analysis module. To decrease the influence from non-vegetated land, we defined the thresholds to mask out non-vegetated pixels like water and impervious surfaces to reduce the noise from non-vegetation signals in all Landsat images. Then we used the Theil-Sen Median method for trend testing. The Theil-Sen Median method, also known as Sen slope estimation, is a robust nonparametric statistical trend calculation method. Compared with other parametric test methods, it does not require samples to follow a certain distribution and is less disturbed by outliers, so it is more suitable for sequential variables. This method has high computational efficiency and is insensitive to measurement errors and outlier data, and is often used in trend analysis of long-term series data in vegetation and judging the significance (Liu et al., 2019). To explore the long time series of change in vegetation cover, we separated the time series data into four periods: 1990–2020, 1990–2000, 2000–2010, and 2010–2020, and obtained the mean NDVI and NDVI change trend figures, respectively.

The specific calculation process is as follows:

$$z = \begin{cases} \frac{s}{\sqrt{Var(s)}} & (s > 0) \\ 0 & (s = 0) \\ \frac{s+1}{\sqrt{Var(s)}} & (s < 0) \end{cases} \quad (3.1)$$

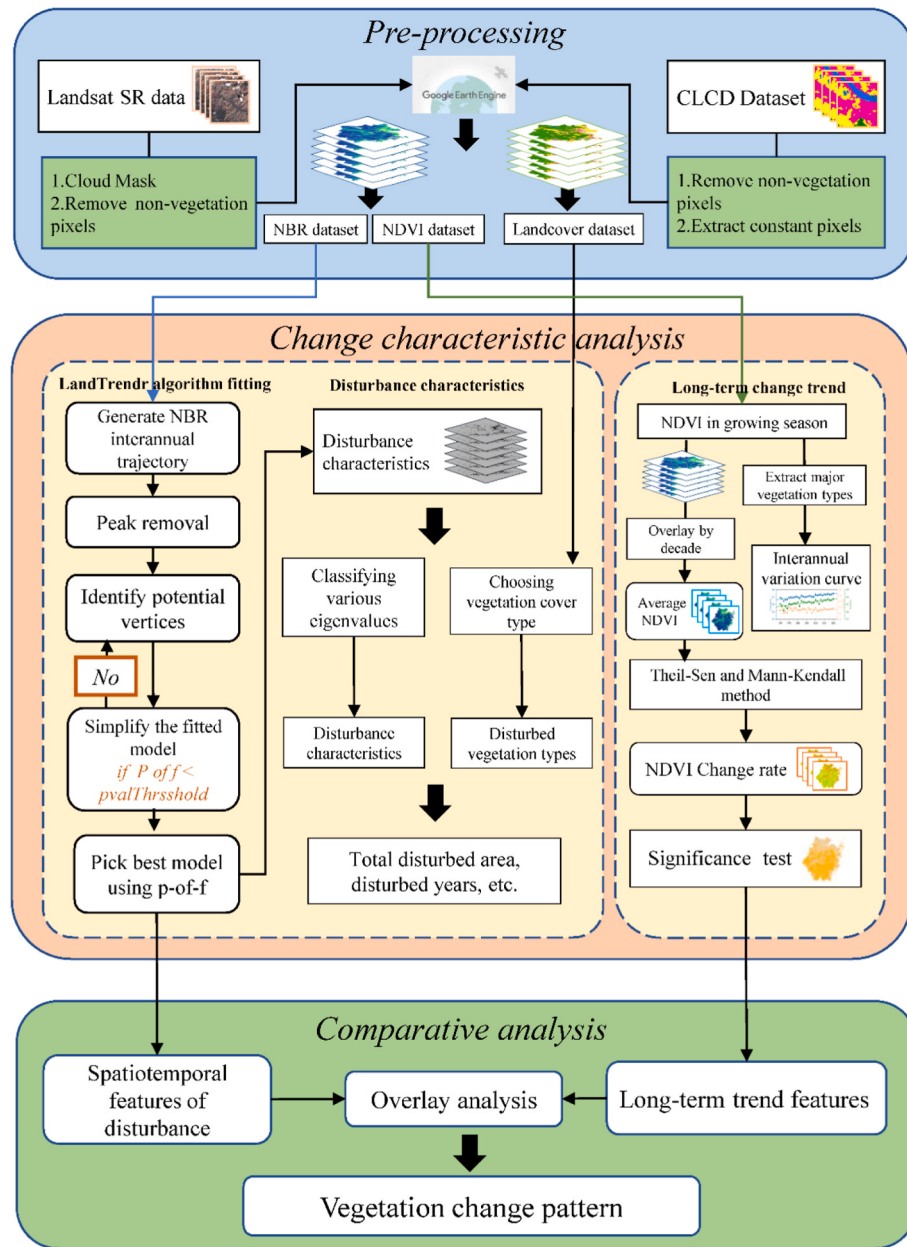


Fig. 2. The flow chart of this research.

$$s = \sum_{i=1}^{n-1} \sum_{j=i+1}^n \text{sign}(x_j - x_i) \quad (3.2)$$

$$\text{sign}(x_j - x_i) = \begin{cases} 1 & (x_j - x_i > 0) \\ 0 & (x_j - x_i = 0) \\ -1 & (x_j - x_i < 0) \end{cases} \quad (3.3)$$

where Z represents the statistical value of the standardized test, S represents the statistical value of the test, $\text{Var}(S)$ represents the variance, $\text{sign}()$ represents the sign function, and n represent the numbers of data, x_j and x_i present time series data.

The indicator to measure the trend is β , and the formula is shown as follows:

$$\beta = \text{median}\left(\frac{x_j - x_i}{j - i}\right) \forall j < i \quad (3.4)$$

when β is greater than 0, the time series shows an upward trend; when β

is less than 0, the time series shows a downward trend.

2.3.2.2. Change detection module. The LandTrendr algorithm (Kennedy et al., 2010) was used to identify the short-term changes in this study. The main process includes using a set of spectral time segmentation algorithms that could take a single view, such as a band or an index, from the spectral history and go through a process to identify breakpoints that separate persistent changes or periods of stability in spectral trajectories and record the occurrence year of change. It can be used for change detection in time series and to generate data that is largely free of interannual signal noise, and trace-based spectral time series. As a time-series segmentation algorithm, it can be used for change monitoring in time series of medium resolution satellite imagery as well as to generate trajectory-based spectral time series data essentially free of interannual signal noise, thus image-by-image Meta-analyzing time series spectral values to capture long-term, gradual or short-term sharp changes in time series. LandTrendr was originally implemented in IDL (Interactive Data Language), but with the help of engineers at Google, it

has been portable to the GEE platform. The original paper describes the effects and sensitivity of changing some of these argument values. One of the great things about having LandTrendr in GEE (LT-GEE) is that parameter settings are easy and fast to iterate through to find the best set (<https://emapr.github.io/LT-GEE/lt-gee-requirements.html>).

In the disturbance detection part, we used the NBR index which was applied to identify the rapid disturbances. The main steps were: 1) removing noise-induced spikes from the time series, identifying potential vertices, 2) fitting trajectory for the entire period, reducing the segments to simplify the trajectory model, 3) determining the best model and filtering the change in vegetation cover (Yang et al., 2018). LandTrendr requires has a variety of parameters to control the allowable temporal relationships of the final model, which is shown in Table 1. In this study, we adopted default values for the parameters which were proposed by Kennedy and had been verified for accuracy. According to the study (Kennedy et al., 2018), when these parameters were used, LT-GEE and LT-IDL agreed on the number of segmentation vertices in the majority of pixels in all six various types of study regions, and the mean absolute error showed high agreement between the two versions of the algorithm, which means these two have a high degree of agreement, and the parameters are suitable for LT-GEE. Moreover, numerous studies had used these parameters (Cohen et al., 2018; Rodman et al., 2021), which proves this set of parameters is suitable for forest change detection. Therefore, we adopted default values for the parameters in this study (Table 1).

After that, we used the samples derived from the TimeSync application to verify the result. TimeSync is the conventional way of verifying LandTrendr segmentation and resulting disturbance maps. It adheres to the same spectral-temporal vertex and segmentation paradigm as LandTrendr and was created as a complement to it. We randomly generated 400 points in the land area of Zhejiang Province (Fig. S3). Since some samples cannot be labeled because of data gaps, we remained 384 valid points. All samples were manually interpreted through TimeSync, we calculate the overall accuracy of our method by comparing its results with samples, an example is shown in Fig. S4. Finally, the accuracy reaches 82.55%, which proves that this result has a relatively high degree of credibility (Table 2).

2.3.3. Comparative analysis

Through the implementation of the framework, we obtained the long-term trend features and the short-term disturbance characteristics. As for the long-term trend features, the trends and average spatiotemporal distributions of the NDVI for study areas were derived in four periods: 1990–2020, 1990–2000, 2000–2010, and 2010–2020. Especially, since the focus of this research was on vegetation changes, and the study region has been covered by large areas of forest and cropland (95%), shrubs, grasslands, and wetlands could be neglected. We had only conducted a more in-depth analysis of forest and cropland by choosing 30-year constant forest pixels (hereinafter referred to as forest) and cropland pixels (hereinafter referred to as cropland) based on the CLCD dataset. These pixels were selected to explore the changes in the areas where anthropogenic interference was weak, and the curves of forest and cropland are screened out after calculating the NDVI of total vegetation in the province.

As for the short-term disturbance characteristics, the spatiotemporal

Table 1
The parameters used in this study.

Parameter	Typical values	Coefficient
Max Segments	6 to 10	6
Spike Threshold	0.75 to 10	0.9
Vertex Count Overshoot	3	3
Recovery Threshold	0.25 to 1.0	0.25
P-value Threshold	0.05 to 0.15	0.05
Best Model Proportion	0.75 to 0.90	0.75
Min Observations Needed	6 to 10	6

Table 2
The result of verification.

Estimated	Interpreted		Total	Commission error
	Disturbance	No disturbance		
Disturbance	101	26	127	20.47%
No disturbance	41	216	257	15.95%
Total	142	242	384	
Omission error	28.87%	10.74%		
Overall accuracy	82.55%	F1 score = 0.75		

variation of vegetation disturbance can be further analyzed after obtaining the vegetation disturbance characteristics: the occurrence location, occurrence time, and the frequency of disturbance in the same area by the LandTrendr algorithm. We superimposed the above data with the contemporaneous CLCD data to evaluate the disturbance features within different vegetation types.

Finally, we compared the two features (i.e., the long-term trend features and short-term disturbance characteristics) in combination to achieve a comprehensive characterization of the vegetation changes.

3. Results

3.1. The spatiotemporal characterization of the vegetation

The average annual growing season NDVI during in study period is displayed below for different periods (Fig. 3). The results show that the higher NDVI regions are distributed in the south and the west of the study area which are mountainous areas, whereas the lower NDVI values concentrated on the plains and coastal area. Meanwhile, NDVI in mountains rose gradually from 1990 to 2020; in contrast, the NDVI in the plain area consistently declined, and the gap between the two widened with time. The areas with low NDVI values (0.2–0.3) were mostly distributed around highly urbanized areas like Hangzhou, Ningbo, and Wenzhou. Moreover, the acreage of low NDVI area was growing with the year, notably in the northern Zhejiang plain.

The NDVI values of vegetation, forests, and cropland are also subjected to trend analysis (Fig. 4). During the study period, the NDVI of vegetation increased slowly from 0.69 in 1990 to 0.75 in 2020, with little fluctuation in the process. The change in the forest was more pronounced, with a relatively high growth rate. In contrast, cropland had a significant fluctuation from 1990 to 2010 and then remained stable until 2020. Since 2014, the three curves had mainly stayed steady, with cropland in low values and forests in high values. It should be noted, we found low values for the years 1992 and 2001 while analyzing the NDVI curves. After reviewing the original data, we conclude that the inaccuracy was caused by missing data within the images in those years caused by the cloud. The months with higher vegetation NDVI values had relatively more cloud cover, so a smaller value was used in the final synthesis of the max value of the growing season.

3.2. The trend of vegetation during the period

The changing trend of NDVI is depicted below (Fig. 5). The areas with enhanced NDVI were mainly in mountainous areas, while the areas with reduced NDVI were mainly located in plains. The NDVI in mountainous areas remained in an increasing state ($\text{slope} > 0$) during the study period, with the maximum growth occurring from 1990 to 2000. Thereafter, NDVI in mountainous area growth rate started to slow down. The majority of the regions with visible NDVI declined were located in the plains ($\text{slope} < -0.01$), and the greatest reduction occurred between 2000 and 2010. We took the spatiotemporal changes of the NDVI decline area in the northern plain as an example. Between 1990 and 2000, only Hangzhou and some areas connected to its southern part had an apparent NDVI decline ($\text{slope} < -0.015$), then the area expanded outward to Jiaxing, Huzhou, finally covering the entire northern Zhejiang

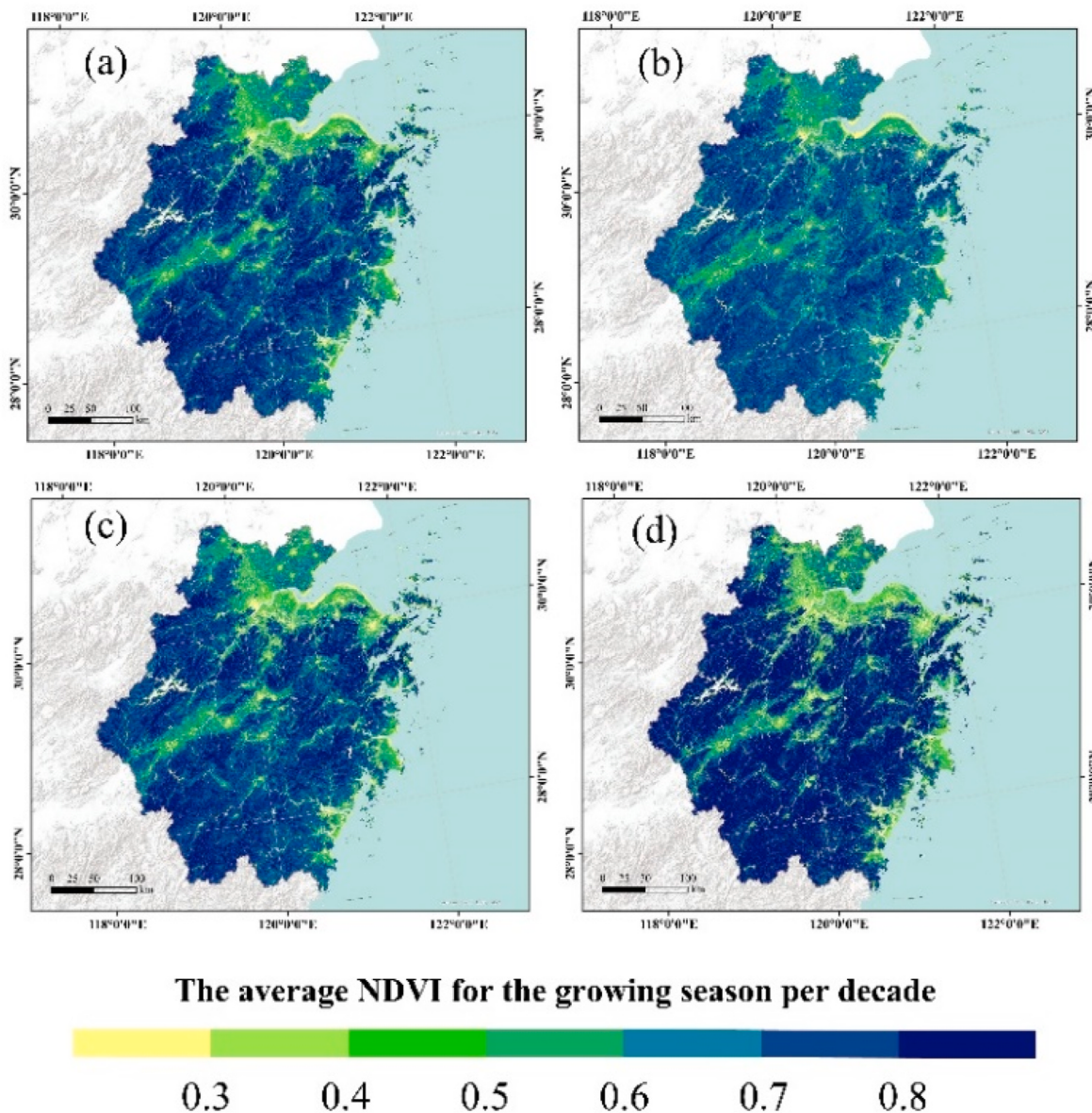


Fig. 3. Spatial pattern of average annual growing season NDVI during 1990–2020 (a), 1990–2000 (b), 2000–2010 (c), and 2010–2020 (d), respectively.

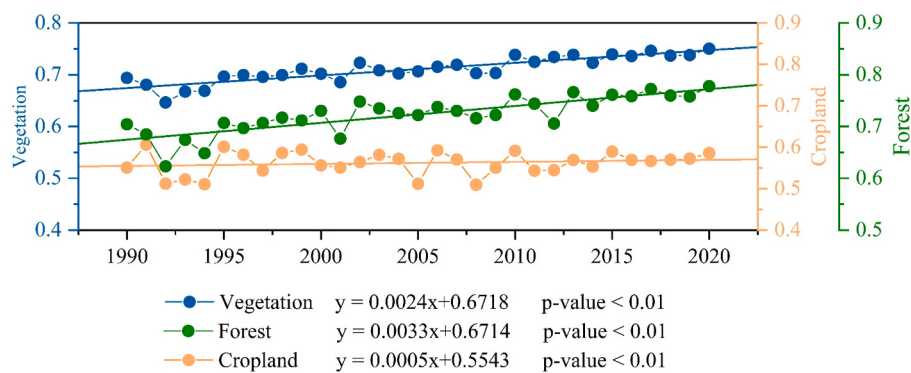


Fig. 4. Interannual changes in NDVI for all vegetation, cropland, and forest in Zhejiang Province from 1990 to 2020, respectively.

Plain. After that, the scope of the area started to shrink, with almost no area in the south of Hangzhou where NDVI declined. Additionally, we conducted a significance test, and the outcomes demonstrated that this

study was statistically significant ($p < 0.05$) in most areas of the study areas.

Through the analysis of Figs. 3–5, we conclude that the vegetation in

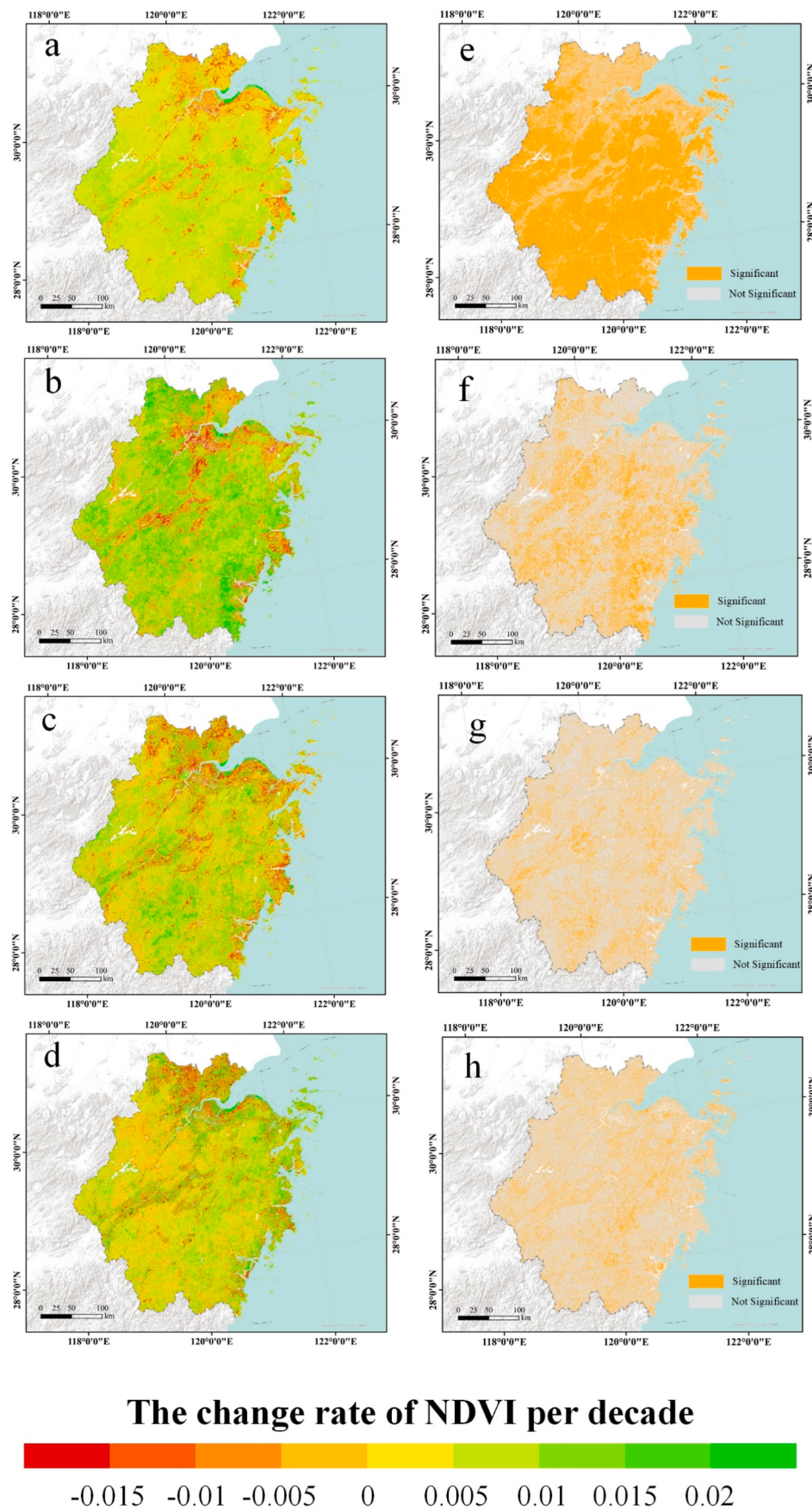


Fig. 5. The trend in mean growing season NDVI for 1990–2020 (a), 1990–2000 (b), 2000–2010 (c), and 2010–2020 (d), respectively, and the significance of the trend analysis for 1990–2020 (e), 1990–2000 (f), 2000–2010 (g), and 2010–2020 (h), respectively.

Zhejiang Province kept greening during the study time in general, and the NDVI of total vegetation rose slowly, but the variation trend had obvious divergences in various regions. In subdivisions, the forest in the mountains had good growth, and the NDVI rose gradually. The vegetation in the plain, especially around cities had declined seriously, and the area where NDVI decreased first increased and then decreased within the study period, and the gap of NDVI value between the mountains and plains continued to enlarge.

3.3. The disturbance characterization

The distributions of vegetation disturbances between 1990 and 2020 in the study region are presented in Fig. 6. The disturbed areas occupied 42.28% of the study region's area (66.92% of vegetation coverage) which were primarily concentrated in established industrialized areas in plains. The minimum disturbance frequency was one time while the maximum frequency was six times in study areas; the ratios for one disturbance time to six disturbance times were 68%, 24%, 5%, 0.8%, 0.08%, and 0.003%, respectively. The areas with less than two disturbance times accounted for 93% of all disturbance areas. Additionally, we calculated the total disturbance area of each county during the study period, and the results showed that disturbances were mainly concentrated in the northern plains and the southeast coast.

The onsets of vegetation disturbances are shown in Fig. 7. We found that the onsets of vegetation disturbances in the northern regions are earlier than the southern regions, while that around the urban area (Fig. 7L1 and 7L2) are earlier than that around the suburban area (Fig. 7L3). For instance, most of the disturbances in downtown Hangzhou happened before 2003 when the majority of which in Lishui occurred after 2006. The disturbance in the downtown area always occurred earlier than that in the suburb, meaning that it usually spreads from the center to the suburb in the same city. This is congruent with the development of various cities in Zhejiang Province, namely Hangzhou, Wenzhou, and Ningbo developed earlier; Quzhou and Lishui evolved later, further supporting the notion that urbanization triggers the greenness increase.

As Fig. 8 shows, there were two peaks in the annual vegetation disturbance area: one around 2003 and the other around 2013, and the disturbance mostly appeared in cropland and forest. It is worth noting that, although the total area of forest and cropland in Zhejiang Province varies greatly, the annual disturbance area was almost the same in the study period, and even in many years, such as 1993 and 2001, the total disturbed area of cropland exceeded that of the forest (Table S1).

4. Discussion

4.1. Comparative analysis of long-term change trends

Many algorithms were only designed to detect one single change

over a period of time, so efficient frameworks with the capability of characterizing multiple landscape changes are attracting more and more attention (Zhu, 2017). In this regard, we proposed a framework that could integrate different vegetation change characteristics. As expected, the long-term change trends and the short-term change features over the study region were presented with the help of the developed framework.

The long-term change trends of vegetation in Zhejiang Province differed spatially and temporally. The results showed that the NDVI of vegetation rose slowly and stably during the whole study time especially after 2010 (Figs. 3 and 4), indicating that the vegetation in Zhejiang Province had a greening trend during the study period, which is different from the previous study (He et al., 2012). They believed that the NDVI of the annual maximum vegetation in Zhejiang Province experienced a steadily declining trend, and the significantly reduced regions were mainly distributed in the typical evergreen broad-leaved forest area from 1990 to 2010. This may be related to the difference in the spatial resolution of images. The spatial resolution of the images they used was 8 km which was relatively coarse for regional or local studies, and they used annual average NDVI rather than growing season NDVI, resulting in susceptibility to interference from clouds. In comparison, the spatial resolution for the data used in this study was 30 m, which can detect the land change processes at a finer scale (Yin et al., 2018). Meanwhile, according to the analysis of the NDVI change curves, forest rather than cropland dominated the changes in vegetation (Fig. 4). This, however, differs from an earlier study that mentioned the shared contribution of cropland and forests to the greener in China's vegetation (Chen et al., 2019). Through further analysis, we believe that this is related to agriculture production practices. The findings of Chen represent a generalization of vegetation changes over all of China, but the scale of agricultural production is generally smaller due to the limitations of terrain in Zhejiang Province. According to the Zhejiang Statistical Yearbook, grain production decreased from 1.6 to 0.6 million tons when the production of goods with a high economic value, like tea and fungus, kept increasing. The study period. It indicates that the agriculture structure has changed in Zhejiang Province, steadily moving away from the conventional planting business.

Additionally, the greening vegetation were mainly concentrated in the mountainous regions, while browning vegetation were distributed in the plains and southeast coast, especially around the cities (Fig. 5). This phenomenon can be interpreted as the nonnegligible effects of human activity on the long-term trends in vegetation, which is also mentioned in the study of He et al. (2020). Moreover, a study emphasized that in the economically developed coastal areas of Zhejiang, a large number of abandoned lands have appeared in the countryside (Wu and Yu, 2001), which is consistent with our analysis of changes in the NDVI of cropland. The tendency of vegetation greening was most obvious between 1990 and 2000 (Fig. 5(b)) compared with other periods. We believed it was a policy-driven result in Zhejiang Province. According to statistics from the National Forestry and Grassland Administration, after Zhejiang

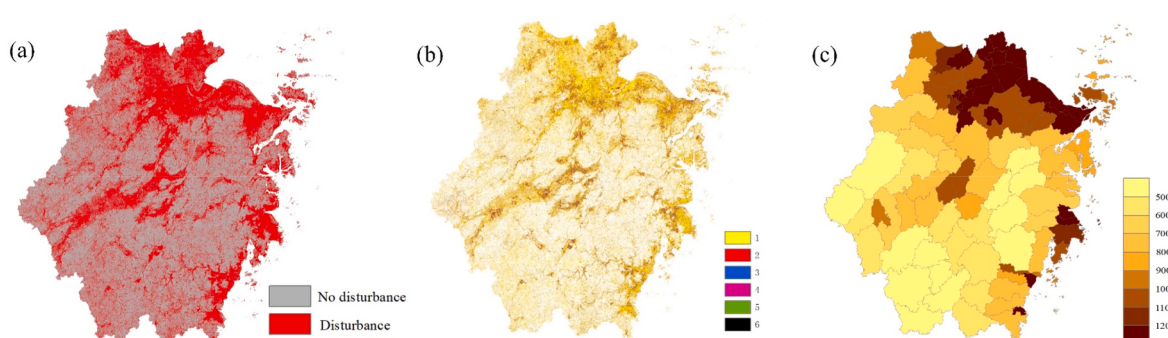


Fig. 6. The occurrence of vegetation disturbances across the study area (a), the spatial distribution of the times of occurrence of vegetation disturbance (b), and the total disturbed area of each county-level district from 1990 to 2020 (c).

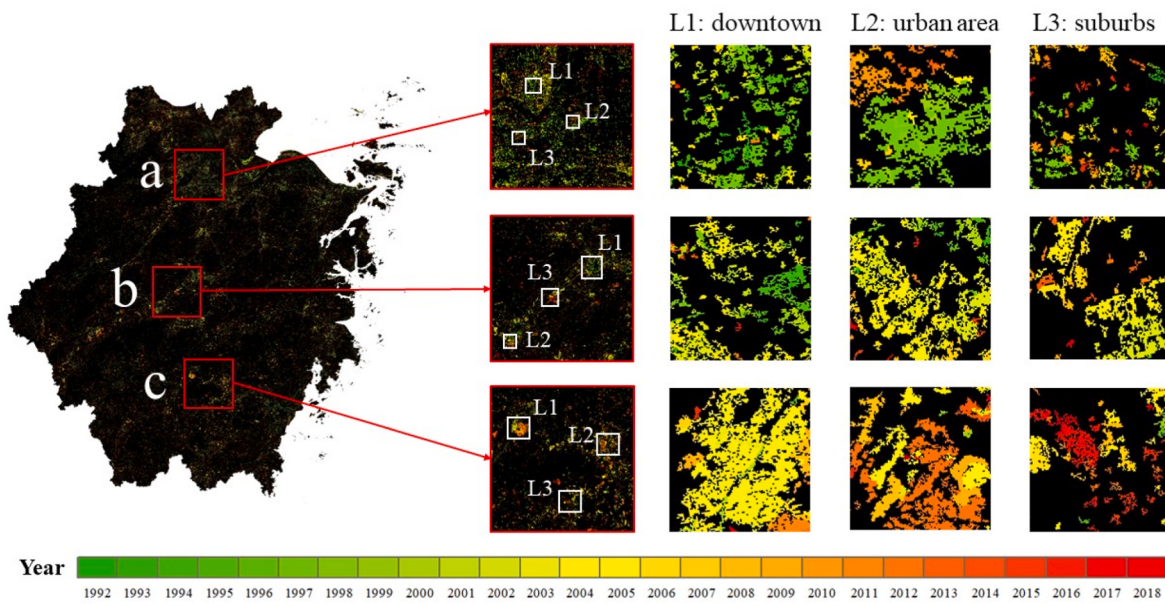


Fig. 7. The time when the disturbance occurred.

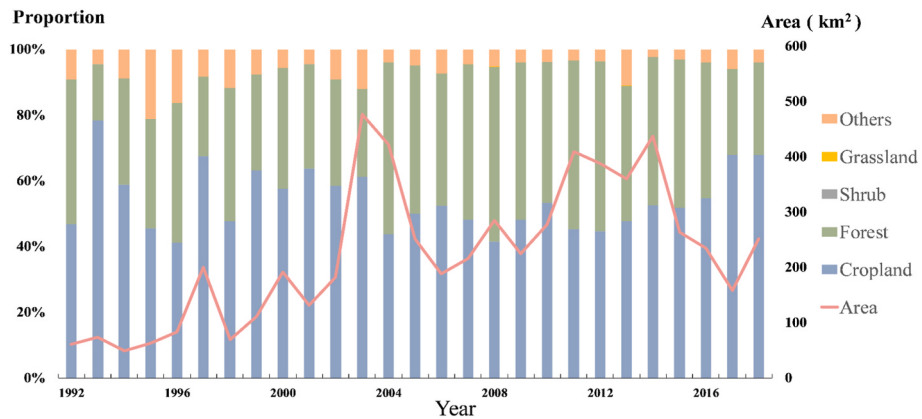


Fig. 8. Areas of disturbed vegetation each year and the proportions of disturbed areas in different vegetation types.

Province announced its goal to *Green Zhejiang in Ten Years* in 1989, the overall area planted in afforestation throughout ten years was 9348 square kilometers, which has led to a remarkable increase in the forest quality. Afterwards, the rate of vegetation greening began to slow as the growth becomes saturated, which is also reflected in the research of He et al. (2013).

In general, with the support of policies, vegetation in Zhejiang Province has grown well over the past 30 years, despite the effect of human causes like urbanization (Cao et al., 2018; Xu et al., 2022; Zhang et al., 2022).

4.2. Disturbance result comparison and attribution analysis

The aforementioned conclusions are based on describing the vegetation in the study region as a whole, and the disturbance features generated by this framework can provide additional insights toward a complete understanding of vegetation dynamics. This framework can emphasize the disturbed areas of various plant types, the interannual variation trend, and the frequency of disturbances in different regions, which is a useful addition to the circumstances that the long-term trend cannot capture.

The disturbance features show that there were numerous vegetation disturbances in the study area accompanied by a lower recurrence rate

of disturbance, which was not reflected in the long-term trend. The northern plain showed the most obvious trend in vegetation deterioration, whereas the southern mountains exhibited the most pronounced trend in vegetation greening. This conclusion is consistent with the study of Song (Song et al., 2021). The disturbances mainly occurred around plains and coastal areas, which further indicated that the development of urbanization has an impact on vegetation. A previous study also obtained similar results (Dong et al., 2017), and we explain the issue in more depth in this study. As mentioned in the policy issued by the Zhejiang Provincial Department of Agriculture and Rural Affairs, there is a very substantial issue with land abandonment in Zhejiang Province (Jin et al., 2022). In addition, reclamation is common in the study region. Since the mid-1980s, the speed of reclamation near Hangzhou Bay has been getting faster, and the reclamation of tidal flats has become the main source of cultivated land and construction land in Zhejiang over the past four decades (Ma, 2012). Specially, reclaimed land will undergo a transition from wasteland to useable land, and continuous transitions between agricultural land, industrial land, and urban construction land, which explains why the high frequency of recurrent disturbance is dispersed in coastal areas. The total disturbed area of different county-level districts we obtained (Fig. 6(c)) can reflect the regional characteristics of vegetation disturbance more clearly. The results could meet the requirements for assessing the ecological

vegetation changes in local areas such as cities and counties, which was raised by He et al. (2020). Meanwhile, this result will provide a reference for the formulation of subsequent ecological civilization construction policies.

As for the changes in different vegetation types (Fig. 8), we found the total disturbed area in the farmland is larger than that in the forest, and there were two peaks of disturbance: 2003 and 2012.

The disturbance peak in 2003 may be induced by an unusual climate. The records of the National Climate Center show that the 2003 high-temperature weather in southern China was abnormal for the period due to its broad range, extended duration, and high temperature, this view is also supported by a previous study (Bai et al., 2010). Moreover, the disturbance peak in 2003 may also be related to the policy implementation. Zhejiang initiated the *Ten Thousand Project* in 2003 to enhance the rural ecological environment in response to the *dirty, chaotic* state of the rural environment as well as the uneven and uncoordinated growth of urban and rural regions. Farmland transformed into roads, and houses, which may also be the cause of the extensive vegetation disturbance that occurred in 2003. Under the double influence of the two, the vegetation in Zhejiang Province has been disturbed in a large area.

In addition, the disturbance peak in 2012 was probably determined by the development policies of Zhejiang Province in recent years and the cropland conversion. As for the policy reason, Gao (2015) believed Zhejiang has accelerated rural construction since 2011, and rural areas have transitioned from being dominated by primary industries to tourism service industries and other tertiary industries, which led to the destruction of the vegetation in the countryside. As for the cropland conversion, the data from the Zhejiang Provincial Bureau of Statistics at the same time demonstrated that from 2011 to 2014, fruit production in Zhejiang Province increased while grain production continued to fall, supporting the trend of cropland conversion. Meanwhile, another possible reason is that Zhejiang Province suffered from continuous meteorological disasters during this period, which therefore increase the possibility of disturbance in vegetation. The Hangjiahu plain, which has the highest concentration of agriculture in Zhejiang Province, was adversely affected by the strong wind, and floods. This resulted in significant agricultural losses in several counties and towns, both the greenhouse infrastructure and the crops in the shed were destroyed, which caused a serious blow to the underdeveloped agriculture in Zhejiang Province (Table S2). The above reasons contributed to the peak of cropland disturbance in 2012.

The results of various trends under our framework exhibit a high degree of temporal and geographical coincidence after a comparison examination of the data. The results of the framework are in line with both policy and real-world circumstances. Zhejiang Province is a developed area with intensive economic and cultural activities, as well as ecological restoration. From this study, relatively common vegetation change characteristics and causes in the eastern coastal areas of China can therefore be deduced. Urbanization construction, reclamation and other reasons can also explain the disturbances in other similar areas.

4.3. Deficiencies and prospects

Although the spatial vegetation changes derived from the LandTrendr time-series approach provide relevant spatiotemporal references for understanding vegetation cover changes in large areas, there are still several points that this study can be improved. Firstly, although the Landsat satellite products were preprocessed, there were still a lot of missing numbers in some years due to cloud cover. In addition, the CLCD dataset is not completely accurate (Yang and Huang, 2021). In response to the aforementioned questions, the following aspects could be improved. Firstly, the multi-source remote sensing data can be combined to complement each other (Hermosilla et al., 2019). For example, summertime cloud-free images of the years before and after can be combined to obtain one or more scene images that can be used to

monitor vegetation coverage and disturbance. Secondly, the accuracy of the results will be increased by applying the machine learning approaches with event-based training samples which could be interpreted from historical high-resolution images.

Additionally, we envision adding a driver analysis module in subsequent studies to dive deeper into the causes of disturbances and use changes in vegetation to indicate the impact of climate change and human activities on terrestrial ecosystems.

4.4. The advantage, implication and innovation of the framework

As Kennedy mentioned, change is not simply a contrast between conditions at two points in time, but rather a continual process operating at both fast and slow rates on landscapes (Kennedy et al., 2018). A joint analysis of long-term trends and short-term disturbances is required if vegetation change is to be fully understood, and there are certain limitations in studying short-term disturbances or long-term trends in isolation. By comparing Figs. 5 and 6(b), we can explain this more clearly: Fig. 5 reflects the change of vegetation NDVI in Zhejiang Province, which can roughly show the growth of vegetation in different regions. However, if we only analyze the long-term change trend of vegetation, we will not be able to accurately locate when the vegetation has changed and how severe it is; similarly, Fig. 6(b) reflects the frequency of vegetation disturbance, and the vegetation disturbance information is analyzed, we can obtain the specific location and year of the disturbed vegetation in the study area, but we cannot obtain the overall greening or browning of the vegetation. But by combining the two, we can summarize the frequency and intensity of disturbances in different regions, which can also represent the impact of human activities and ecosystem changes on vegetation in different regions. With the use of this framework, the divergence between long-term trends and abrupt disturbances in the existing studies on vegetation change could well be resolved, and new approaches to the study of vegetation change can be suggested.

4.5. Results and applications

The results of this study could show the effects of various environmental protection measures put in place in Zhejiang Province over the last 30 years and offer a convincing explanation for several environmental issues and phenomena that took place there. For example, the second phase of the “Natural Forest Resources Protection Project” was started by the Zhejiang Provincial Government in 2015, and the outcomes of its execution are reflected in the forest change analysis and disturbance characteristics of this framework. Fig. 4 shows that after 2016, the vegetation in Zhejiang Province, especially the growth of forests, was in good condition. From Fig. 8, it can be seen that the proportion of forest disturbances decreased in Zhejiang Province during the same period obviously. It is confirmed that this policy has achieved better results. At the same time, the disturbance characteristics can accurately describe and quantify the land changes brought about by urbanization in Zhejiang Province, allowing decision-makers to formulate different environmental protection policies according to the development of different regions. For example, the results of this framework show that a large part of the disturbance in Zhejiang Province occurs in farmland, which is also consistent with the relatively serious land abandonment problem in Zhejiang Province.

Therefore, we have reason to believe that the vegetation changes reflected in this framework are related to the ecological and environmental problems in the study area and could help to guide and formulate future ecological and environmental policies in the province of Zhejiang.

5. Conclusion

In this study, we developed a novel framework for the comprehensive characterization of vegetation changes, including long-term trends

and short-term features. Based on this framework, we obtained the characteristics of vegetation changes in Zhejiang Province, which can be summarized below. The vegetation has been greening gradually in the mountainous regions and has been browning in the plains. Meanwhile, the disturbance also started earlier in the urban center region of Zhejiang Province than it did in the suburban area, and it started earlier in the northern section of the province than in the southern part. Most vegetation disturbances occurred around the built-up areas, and the frequencies of disturbance for most regions were less than two times. Most of the results derived from this study were echoed by previous studies, indicating that the developed framework has a high degree of reliability.

The framework is effective at capturing both the long-term trends and short-term changes of vegetation at a fine scale by using Landsat images. The combination of two change characteristics, with the support of this framework, completely describes the vegetation change in the study area. We expect that the characterization of vegetation change trends based on the framework will be helpful to vegetation science researchers, managers, and decision-makers who conduct ecological environment monitoring and research related to sustainable development.

Author contributions statement

Hancheng Guo: Conceptualization, Methodology, Writing - Original Draft. **Yanyu Wang:** Software, Methodology, Writing - Original Draft. **Jie Yu:** Gave a lot of suggestions in the article revision stage, data collection. **Lina Yi:** Resources, Visualization, Writing - Review & Editing. **Zhou Shi:** Project administration, Formal analysis, Funding acquisition. **Fumin Wang:** Formal analysis, Review & Editing, Funding acquisition.

Declaration of competing interest

The authors declare that they have no known competing financial interests or personal relationships that could have appeared to influence the work reported in this paper.

Data availability

Data will be made available on request.

Acknowledgements

This work was supported by the Key R&D Program of Zhejiang (2022C03078), and the Science and Technology Innovation Leading Talent Program of Zhejiang Province (2019R52004).

Appendix A. Supplementary data

Supplementary data to this article can be found online at <https://doi.org/10.1016/j.envres.2023.115379>.

References

- Bai, Y., Zhi, X., Qi, H., Zhang, L., 2010. Severe drought monitoring in south China based on the standardized precipitation index at different scales. *Sci. Meteorologl. Sin.* 30, 292–300.
- Benedict, T.D., Brown, J.F., Boyte, S.P., Howard, D.M., Fuchs, B.A., Wardlow, B.D., Tadesse, T., Evenson, K.A., 2021. Exploring VIIRS continuity with MODIS in an expedited capability for monitoring drought-related vegetation conditions. *Rem. Sens.* 13 (6).
- Bueno, I.T., McDermid, G.J., Silveira, E.M.O., Hird, J.N., Domingos, B.I., Junior, F.A.W., 2020. Spatial agreement among vegetation disturbance maps in tropical domains using landsat time series. *Rem. Sens.* 12.
- Cao, L.D., Li, J.L., Ye, M.Y., Pu, R.L., Liu, Y.C., Guo, Q.D., Feng, B.X., Song, X.Y., 2018. Changes of ecosystem service value in a coastal zone of Zhejiang province, China, during rapid urbanization. *Int. J. Environ. Res. Publ. Health* 15.
- Chen, C., Park, T., Wang, X.H., Piao, S.L., Xu, B.D., Chaturvedi, R.K., Fuchs, R., Brokvkin, V., Ciais, P., Fensholt, R., Tommervik, H., Bala, G., Zhu, Z.C., Nemani, R.R., Myneni, R.B., 2019. China and India lead in greening of the world through land-use management. *Nat. Sustain.* 2, 122–129.
- Cohen, W.B., Yang, Z.Q., Heale, S.P., Kennedy, R.E., Gorelic, N., 2018. A LandTrendr multispectral ensemble for forest disturbance detection. *Rem. Sens. Environ.* 205, 131–140.
- Danneyrolles, V., Dupuis, S., Fortin, G., Leroyer, M., de Romer, A., Terrail, R., Vellend, M., Boucher, Y., Lafamme, J., Bergeron, Y., Arseneault, D., 2019. Stronger influence of anthropogenic disturbance than climate change on century-scale compositional changes in northern forests. *Nat. Commun.* 10, 7.
- Dong, C.-w., Cao, Y., Tan, Y.-z., 2017. Urban expansion and vegetation changes in Hangzhou Bay area using night-light data. *Yingyong Shengtai Xuebao* 28, 231–238.
- Fang, X.Q., Zhu, Q.A., Ren, L.L., Chen, H., Wang, K., Peng, C.H., 2018. Large-scale detection of vegetation dynamics and their potential drivers using MODIS images and BFAST: a case study in Quebec, Canada. *Rem. Sens. Environ.* 206, 391–402.
- Foga, S., Scaramuzza, P.L., Guo, S., Zhu, Z., Dilley, R.D., Beckmann, T., Schmidt, G.L., Dwyer, J.L., Hughes, M.J., Laue, B., 2017. Cloud detection algorithm comparison and validation for operational Landsat data products. *Rem. Sens. Environ.* 194, 379–390.
- Fu, B.L., Lan, F.W., Yao, H., Qin, J.L., He, H.C., Liu, L.L., Huang, L.K., Fan, D.L., Gao, E.R., 2022. Spatio-temporal monitoring of marsh vegetation phenology and its response to hydro-meteorological factors using CCDC algorithm with optical and SAR images: in case of Honghe National Nature Reserve, China. *Sci. Total Environ.* 843, 18.
- Gao, C., 2015. Research on Innovation of Producer Service Industry in Zhejiang Province Based on the Perspective of Big Data. *Market Modernization* 28, 142–143.
- Ge, W.Y., Deng, L.Q., Wang, F., Han, J.Q., 2021. Quantifying the contributions of human activities and climate change to vegetation net primary productivity dynamics in China from 2001 to 2016. *Sci. Total Environ.* 773.
- He, Y., Fan, G., Zhang, x., Li, Z., Gao, D., 2013. Vegetation phenology change and its response to climate change in Zhejiang Province. *J. Nat. Resour.* 28 (02), 220–233.
- He, Y., Fan, G., Zhang, X., Liu, M., Gao, D., 2012. Variation of vegetation NDVI and its response to climate change in Zhejiang Province. *Acta Ecol. Sin.* 32, 4352–4362.
- He, Z., Zhang, Y., He, Y., Zhang, X., Cai, J., Lei, L., 2020. Trends of vegetation change and driving factor analysis in recent 20 Years over Zhejiang province. *Ecol. Environ. Sci.* 29, 1530–1539.
- Hemati, M., Hasanlou, M., Mahdianpari, M., Mohammadimanesh, F., 2021. A systematic review of landsat data for change detection applications: 50 Years of monitoring the Earth. *Rem. Sens.* 13.
- Hermosilla, T., Wulder, M.A., White, J.C., Coops, N.C., 2019. Prevalence of multiple forest disturbances and impact on vegetation regrowth from interannual Landsat time series (1985–2015). *Rem. Sens. Environ.* 233, 12.
- Hislop, S., Jones, S., Soto-Berelov, M., Skidmore, A., Haywood, A., Nguyen, T.H., 2019. A fusion approach to forest disturbance mapping using time series ensemble techniques. *Rem. Sens. Environ.* 221, 188–197.
- Holben, B.N., 1986. Characteristics of maximum-value composite images from temporal AVHRR data. *Int. J. Rem. Sens.* 7, 1417–1434.
- Houborg, R., Soegaard, H., Boegh, E., 2007. Combining vegetation index and model inversion methods for the extraction of key vegetation biophysical parameters using Terra and Aqua MODIS reflectance data. *Rem. Sens. Environ.* 106, 39–58.
- Jin, Y.Y., Zhang, B.B., Zhang, H.B., Tan, L., Ma, J.L., 2022. The scale and revenue of the land-use balance quota in Zhejiang province: based on the inverted U-shaped curve. *Land* 11.
- Kennedy, R., Yang, Z., Gorelick, N., Braaten, J., Cavalcante, L., Cohen, W., Healey, S., 2018. Implementation of the LandTrendr algorithm on Google Earth engine. *Rem. Sens.* 10.
- Kennedy, R.E., Yang, Z.G., Cohen, W.B., 2010. Detecting trends in forest disturbance and recovery using yearly Landsat time series: 1. LandTrendr - temporal segmentation algorithms. *Rem. Sens. Environ.* 114, 2897–2910.
- Komba, A.W., Watanabe, T., Kaneko, M., Chand, M.B., 2021. Monitoring of vegetation disturbance around protected areas in Central Tanzania using landsat time-series data. *Rem. Sens.* 13, 18.
- Li, G., Sun, S.B., Han, J.C., Yan, J.W., Liu, W.B., Wei, Y., Lu, N., Sun, Y.Y., 2019. Impacts of Chinese grain for green program and climate change on vegetation in the loess plateau during 1982–2015. *Sci. Total Environ.* 660, 177–187.
- Li, S., Li, C., Kang, X., 2021. Development status and future prospects of multi-source remote sensing image fusion. *J. Rem. Sens.* 25, 148–166.
- Liang, Y.J., Liu, L.J., Hashimoto, S., 2020. Spatiotemporal analysis of trends in vegetation change across an artificial desert oasis, Northwest China, 1975–2010. *Arabian J. Geosci.* 13 (15).
- Lin, X.N., Niu, J.Z., Berndtsson, R., Yu, X.X., Zhang, L., Chen, X.W., 2020. NDVI dynamics and its response to climate change and reforestation in northern China. *Rem. Sens.* 12, 15.
- Liu, Q.H., Wang, X.H., Zhang, Y.L., Zhang, H.M., Li, L.H., 2019. Vegetation degradation and its driving factors in the farming-pastoral ecotone over the countries along belt and road initiative. *Sustainability* 11.
- Liu, Y., Liu, H.H., Chen, Y., Gang, C.C., Shen, Y.F., 2022. Quantifying the contributions of climate change and human activities to vegetation dynamic in China based on multiple indices. *Sci. Total Environ.* 838, 12.
- Ma, R., 2012. Cultural Interpretation of the Evolution of Land Use Modes for Tidal Flat Reclamation and Its Enlightenment to the Design of Oceanic Cities—Taking Zhejiang Province as an Example. *Innovation* 6, 99–102.
- Nguyen, T.H., Jones, S.D., Soto-Berelov, M., Haywood, A., Hislop, S., 2018. A spatial and temporal analysis of forest dynamics using Landsat time-series. *Rem. Sens. Environ.* 217, 461–475.

- Novillo, C.J., Arrogante-Funes, P., Romero-Calcerrada, R., 2019. Recent NDVI trends in mainland Spain: land-cover and phytoclimatic-type implications. *ISPRS Int. J. Geo-Inf.* 8 (1).
- Radocaj, D., Obhodas, J., Jurisic, M., Gasparovic, M., 2020. Global Open Data Remote Sensing Satellite Missions for Land Monitoring and Conservation: A Review. *Land* 9.
- Rodman, K.C., Andrus, R.A., Veblen, T.T., Hart, S.J., 2021. Disturbance detection in landsat time series is influenced by tree mortality agent and severity, not by prior disturbance. *Rem. Sens. Environ.* 254.
- Roy, D.P., Kovalskyy, V., Zhang, H., Vermote, E.F., Yan, L., Kumar, S.S., Egorov, A., 2016. Characterization of Landsat-7 to Landsat-8 reflective wavelength and normalized difference vegetation index continuity. *Rem. Sens. Environ.* 185, 57–70.
- Song, L., Deng, J., Wang, W., Qi, D., 2021. Temporal and spatial variations of vegetation coverage in Zhejiang province based on MODIS data. *J. Yangtze River Sci. Res. Inst.* 38, 40–46.
- Soudzilovskaja, N.A., van Bodegom, P.M., Terrier, C., van't Zelfde, M., McCallum, I., McCormack, M.L., Fisher, J.B., Brundrett, M.C., de Sa, N.C., Tedersoo, L., 2019. Global mycorrhizal plant distribution linked to terrestrial carbon stocks. *Nat. Commun.* 10.
- Tao, X., Huang, C.Q., Zhao, F., Schleeweis, K., Masek, J., Liang, S.L., 2019. Mapping forest disturbance intensity in North and South Carolina using annual Landsat observations and field inventory data. *Rem. Sens. Environ.* 221, 351–362.
- Verbesselt, J., Hyndman, R., Zeileis, A., Culvenor, D., 2010. Phenological change detection while accounting for abrupt and gradual trends in satellite image time series. *Rem. Sens. Environ.* 114, 2970–2980.
- Wang, Y., Guo, C.H., Chen, X.J., Jia, L.Q., Guo, X.N., Chen, R.S., Zhang, M.S., Chen, Z.Y., Wang, H.D., 2021. Carbon peak and carbon neutrality in China: goals, implementation path and prospects. *China Geol.* 4, 720–746.
- Wei, X.H., Li, Q., Zhang, M.F., Giles-Hansen, K., Liu, W.F., Fan, H.B., Wang, Y., Zhou, G.Y., Piao, S.L., Liu, S.R., 2018. Vegetation cover-another dominant factor in determining global water resources in forested regions. *Global Change Biol.* 24 (2), 786–795.
- Woodcock, C.E., Allen, R., Anderson, M., Belward, A., Bindschadler, R., Cohen, W., Gao, F., Goward, S.N., Helder, D., Helmer, E., Nemani, R., Oreopoulos, L., Schott, J., Thenkabail, P.S., Vermote, E.F., Vogelmann, J., Wulder, M.A., Wynne, R., Landsat Sci., T., 2008. Free access to Landsat imagery. *Science* 320, 1011, 1011.
- Wu, S., Yu, Y., 2001. Discussion on Afforestation of Discarded Lands in Coastal Areas. *East China Forest. Management* 02, 25–26.
- Wulder, M.A., Loveland, T.R., Roy, D.P., Crawford, C.J., Masek, J.G., Woodcock, C.E., Allen, R.G., Anderson, M.C., Belward, A.S., Cohen, W.B., Dwyer, J., Erb, A., Gao, F., Griffiths, P., Helder, D., Hermosillo, T., Hippel, J.D., Hostert, P., Hughes, M.J., Huntington, J., Johnson, D.M., Kennedy, R., Kilic, A., Li, Z., Lymburner, L., McCorkel, J., Pahlevan, N., Scambos, T.A., Schaaf, C., Schott, J.R., Sheng, Y.W., Storey, J., Vermote, E., Vogelmann, J., White, J.C., Wynne, R.H., Zhu, Z., 2019. Current status of Landsat program, science, and applications. *Rem. Sens. Environ.* 225, 127–147.
- Xu, X.H., Yu, J., Wang, F.E., 2022. Analysis of ecosystem service drivers based on interpretive machine learning: a case study of Zhejiang Province, China. *Environ. Sci. Pollut. Control Ser.* 29, 64060–64076.
- Yang, J., Huang, X., 2021. The 30 m annual land cover dataset and its dynamics in China from 1990 to 2019. *Earth Syst. Sci. Data* 13, 3907–3925.
- Yang, Y.J., Erskine, P.D., Lechner, A.M., Mulligan, D., Zhang, S.L., Wang, Z.Y., 2018. Detecting the dynamics of vegetation disturbance and recovery in surface mining area via Landsat imagery and LandTrendr algorithm. *J. Clean. Prod.* 178, 353–362.
- Yin, H., Pflegmacher, D., Li, A., Li, Z.G., Hostert, P., 2018. Land use and land cover change in Inner Mongolia - understanding the effects of China's re-vegetation programs. *Rem. Sens. Environ.* 204, 918–930.
- Zhang, X.L., Huang, X.R., 2019. Human disturbance caused stronger influences on global vegetation change than climate change. *PeerJ* 7, 15.
- Zhang, Y.W., Lin, H.L., Ye, G.Q., 2022. Long-term benefits of coastline ecological restoration in China. *J. Mar. Sci. Eng.* 10.
- Zhou, Y., Guo, X., Zou, M., Chen, G., Guo, J., Yue, D., 2019. Study on spatio-temporal variation of vegetation disturbance in the southern part of Tianshui by disturbance index. *Ecol. Sci.* 38, 102–110.
- Zhu, Z., Qiu, S., Ye, S., 2022. Remote sensing of land change: a multifaceted perspective. *Rem. Sens. Environ.* 282.
- Zhu, Z., Woodcock, C.E., 2014. Continuous change detection and classification of land cover using all available Landsat data. *Rem. Sens. Environ.* 144, 152–171.
- Zhu, Z., 2017. Change detection using landsat time series: a review of frequencies, preprocessing, algorithms, and applications. *ISPRS J. Photogrammetry Remote Sens.* 130, 370–384.